06

Pore space parameters and characteristics of SiC ceramic materials

© R.D. Kapustin, A.O. Kirillov, V.E. Loryan

Merzhanov Institute of Structural Macrokinetics and Materials Science Russian Academy of Sciences,
142432 Chernogolovka, Russia
e-mail: kapustin-roman@mail.ru

Received March 12, 2025
Revised May 15, 2025
Accepted May 19, 2025

The work is devoted to the low-temperature synthesis of porous ceramic materials based on finely dispersed SiC with sintering silicon oxide and magnesia binders. Particular attention is paid to the influence of the shape and morphology of the particles of the initial powder components on the structural parameters and characteristics of porous ceramic materials. Silicon carbide-based membranes sintered at maximum temperatures from 1000 °C to 1300 °C had average pore sizes from 0.5 to 1 μm, open porosity up to 50 %, flexural strength up to 48.5 MPa and high water permeability up to 78901 $\cdot$ m^{-2} $\cdot$ h^{-1} $\cdot$ bar^{-1}. The established filtration efficiency was $\sim$ 99 % while maintaining stable permeability and physical and mechanical characteristics after multiple filtration-regeneration cycles. The obtained new knowledge about the influence of the morphology of the initial powders on the parameters of the pore space and the physical and mechanical characteristics of the synthesized porous ceramics expands the possibilities of correct prediction and provision of specified parameters of the structure and properties of materials. The results of this work can be used for the production of porous SiC membranes with high energy efficiency and technological simplicity, highly effective for micro- and ultrafiltration processes, and also having the potential for use as substrates for catalysts.

Keywords: porous ceramics, pore size, porosity, permeability.

DOI: 10.61011/TP.2025.11.62239.34-25

Introduction

Determination of role of the structural and dimensional factor and its influence on the parameters of the pore space and the operational properties of materials and products made from them is an important issue that needs to be addressed in the development of highly efficient ultra- and nanoporous ceramic materials. Establishing the relationship between the structural (morphology of the material, porosity, pore size, etc.) and operational properties (strength, permeability, catalytic properties) of highly porous ceramics makes it possible to successfully solve the problems of creating ceramic filters and permeable catalytic converters for preset operational requirements and characteristics.

In turn, it is obvious that both the macro- and microstructure of the material objectively depends on the properties of the initial components (solid and liquid), as well as on the technological parameters of their preparation: the ratio of filler and binder, pressing pressure, and the evolution of the phase composition during synthesis under the influence of temperatures.

Thus, the selection of initial components with the necessary morphology of the particle surface, the creation of powder mixtures of optimal granulometric composition for synthesis and the selection of formulations of sintering additives are among the determining factors for obtaining porous ceramic materials with the required parameters of the pore space and performance properties. A related area is the search for methods and techniques that can significantly reduce sintering temperatures and increase the energy efficiency of the material production process.

Earlier, we reported in Ref. [1] about the successful synthesis of ceramic membranes based on $Al2O_3$ using SiC, SiO_2 and MgO binders to reduce the sintering temperature to 1300 °C to achieve acceptable mechanical the strength and permeability of the material. It has been shown that SiC oxidation produces an active SiO_2 during sintering, which dissolves the present MgO to form a liquid phase of clinoenstatite composition, strengthening the structure of the material. First of all, the influence of the dimensional characteristics of the initial components on the morphology and characteristics of synthesized materials was studied.

In this paper, the focus of the research direction is shifted to the study of the possibilities of controlling the structural part of the structural-dimensional factor.

The purpose of the research was to study and evaluate the significance of the influence of the morphology of the initial powders on the properties and characteristics of porous permeable ceramics in order to correctly predict and ensure the specified structural, dimensional and physico-mechanical parameters of the materials.

The required parameters depend mainly on the application of the materials and products based on them. Microfiltration of liquids requires materials with effective hydraulic permeability and an average pore size of less than a micrometer. To ensure the efficiency of catalytic processes of combined-cycle gas mixtures, materials with a highly developed surface of the pore space are in demand.

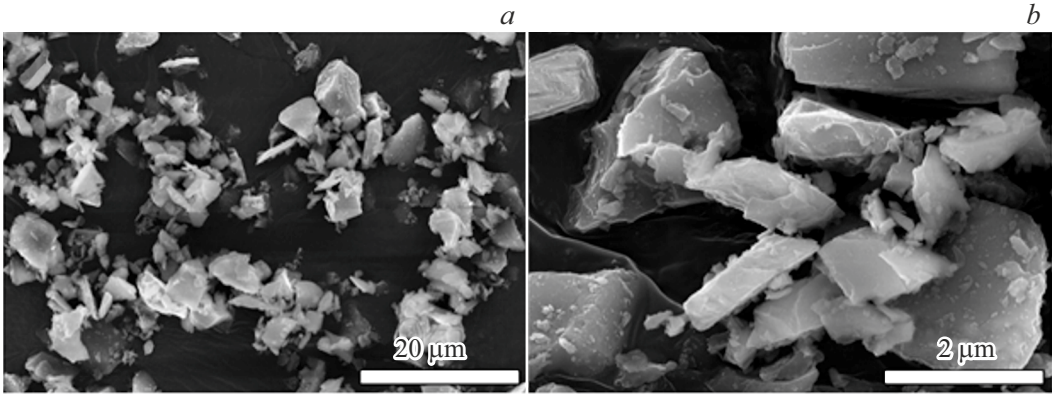

Figure 1. Microstructure of the filler powder SiC_P.

Thus, in order to achieve this goal, it is necessary to evaluate the relationship between the size and morphology of the initial powder components with the structural parameters (porosity, pore size, pore surface development) of the material, as well as with the possibility of achieving the specified operational properties: gas permeability, strength, hydraulic characteristics, etc.

1. Materials and methods of research

For the synthesis of porous ceramics, a multicomponent mixture based on the filler SiC_P (D50:3 μm, LLC „Platinum“, GOST26327-84) obtained by sintering was used in this work (Fig. 1). silica with carbon in an Acheson graphite electric furnace at a high temperature of about 2000 °C: $SiO_2+3C \rightarrow SiC+2CO$.

According to the XRD results, SiC_P powder consists of the modification α-SiC (PDF 2№ 010-72-4531, sp. gr. $P6_3mc$). Specific surface area $\sim 1.2\,m^2/g$.

Based on the results of the microstructure analysis (Fig. 1), it was found that the particles of this powder have a fragmented structure with an irregular geometric shape (a sphericity coefficient of 0.5 was determined). There is also some difference in the size range of the powder particles, which has a bimodal distribution. The average particle size for one mode is 1.38 μm and 9.54 μm for the other mode.

In general, in the framework of the research, the powder had an identical characteristic particle size with the SHS powder SiC_{SHS} from Ref. [2] for the correct comparison of synthesized porous materials based on them. At the same time, the specific surface area of the SiC_P filler used is more than an order of magnitude smaller than the specific surface area of SiC_{SHS}, which allows for a comparative assessment of the effect on the morphology and characteristics of materials, primarily the structural parameters of the initial filler powders.

MgO (D_{50}) was used as sintering and strengthening binders: 3 μm, AO „LenReaktiv“, GOST 4526-75) and SiO_2 (D_{50}:5 μm, AO „LenReaktiv“, GOST 9428-73). The mass ratio of filler powder to sintering additives (SiC:MgO:SiO_2) corresponded to 94:3:3. This ratio was selected experimentally based on the results of previous studies [1,2].

The initial powder components with a total weight of 200 g were placed in a drum with a diameter of 15 cm and a height of 20 cm with stainless steel balls (diameter of 6mm and a total weight of 800 g) and subjected to mixing for 2h at a rotational speed of 30 rpm. Liquid binders (2 % polyvinyl alcohol and liquid glass) were introduced into the resulting charge, after which it was subjected to uniaxial pressing at a pressure of 10 MPa. The obtained disk-shaped experimental samples had dimensions $\varnothing 40\,mm \times 10\,mm$. The experimental samples were subjected to heat treatment in a laboratory chamber electric furnace at maximum temperatures from 800°C to 1300°C for 1 h in an air atmosphere, followed by cooling to room temperature for 5 h.

The structure of the synthesized material was studied by X-ray diffraction with a monochromator on a secondary beam. Step-by-step scanning was performed in the range of $2\theta = 15 - 80^\circ$ (scanning step 0.05°; delay time 6 s). The recorded radiographs were analyzed using the ICCD PDF-2 map database. Full-scale diffraction pattern analysis was performed in JANUARY 2006 using the Rietveld method [3]. The microstructure of the fracture of the samples was analyzed using the SEM method (Zeiss Ultra+, Carl Zeiss) to evaluate the dimensions and form factors of the structural components of porous ceramics. The size of the resulting pores was also determined by the bubble point method according to GOST 26849-86. The open porosity of SiC_P was determined using the hydrostatic weighing method according to the equation

$$\varepsilon = \frac{m_2 - m_1}{m_2 - m_3} \cdot 100\,\%, \qquad (1)$$

where m_1 is the mass of dry membrane, [g], m_2 is the mass of saturated membrane in air, [g], and m_3 is the mass of saturated membrane in water [g].

Microsizer301 granulometric analyzer was used to analyze the particle distribution in the initial powders and permeate (Fig. 2).

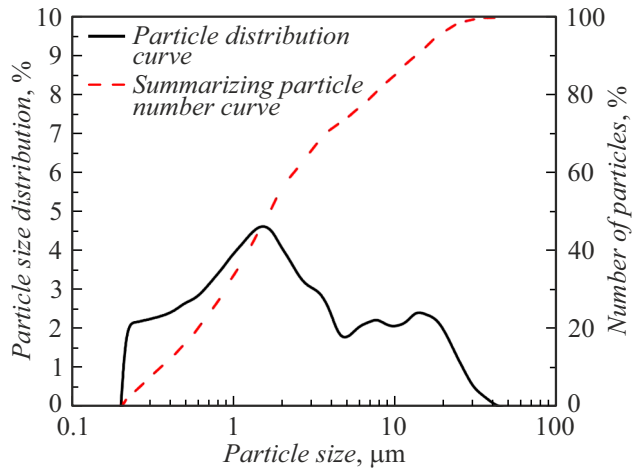

Figure 2. Granulometric composition of SiC_P: powder particle size distribution.

To determine the strength of the samples, the three-point bending method was used on an electromechanical testing machine REM-20 (Metrotest) according to GOST 25282-93. The loading rate was 0.5 mm/min. The strength was calculated using the following formula:

$$\sigma = \frac{3 \cdot P \cdot L}{2 \cdot h^2 \cdot b}, \tag{2}$$

where P is the applied load, [N], L is the distance between supports, [mm], h is the sample height, [mm], b is the sample width, [mm]. Samples with size of $5 \times 5 \times 35$ mm were prepared for strength measurements.

The size of the resulting pores, open porosity, and other parameters of the pore space of the material were determined using an Autopore IV 9500 mercury porosimeter.

Additionally, the gas permeability of porous ceramics was assessed by means of a self-made installation for determining permeability at room temperature using compressed air. The test procedure provided for sealing the samples with a rubber gasket, while measuring the difference between the inlet and outlet pressure. In the case of a laminar flow of a compressible viscous liquid through a porous material, the gas permeability can be found from the Hagen-Poiseuille law.:

$$k = \frac{\eta Q h}{S(P_1 - P_2)} \frac{2P_2}{(P_1 + P_2)}, \tag{3}$$

where k is the permeability, dynamic viscosity η of the air used for calculation is $1.822 \cdot 10^{-5}$ Pa·s, Q is the flow rate, h is the sample thickness, S is the sample cross-sectional area, P_1 and P_2 are the inlet and outlet pressures, respectively. P_1, P_2 and Q were measured using a cascade rotameter system with different measurement limits. For each sample, the permeability was measured at several pressures. The excess inlet pressure increased from 0.02 to 0.2 MPa in increments of 0.01 MPa.

Based on the results of the gas permeability of the samples, the average hydraulic pore sizes of the synthesized materials were calculated according to the method [4]:

$$R = 28.3 \cdot \sqrt{\frac{k}{P_0}}, \tag{4}$$

where k is the sample permeability, [μm^2], P_0 is the open porosity, [%].

The average hydraulic pore size is used to approximate the structure of ceramic materials. The inaccuracy of the estimate is due to the fact that the calculation is carried out assuming that all pore channels are parallel to each other, have a cylindrical shape, a constant cross-section, are perpendicular to the surface and are not tortuous.

The efficiency of separation of the solid and liquid phases of the synthesized SiC_P-membrane was evaluated using a suspension using model SiC powder as the solid phase and distilled water as the liquid phase, respectively. The model powder was introduced into the suspension in an amount of 2 mass% and had a particle size of $D_{50} = 0.5\,\mu m$. Separation experiments were carried out in a cross-flow filtration device at ambient temperature. In this case, the permeability (J, $l \cdot m^{-2} \cdot h^{-1} \cdot bar^{-1}$) of the membrane was measured, which was calculated using the formula (5):

$$J = \frac{V}{S \cdot \Delta P \cdot t} \cdot 100\,\%, \tag{5}$$

where V, [l] is the permeability of pure water through ceramic samples; S, [m^2] is the effective membrane area; t, [h] is the filtration duration, and ΔP is the operating pressure. Three measurements were carried out for samples prepared under the same conditions, and the average values were recorded. The solid residue (R, %) was calculated using the formula

$$R = \frac{C_p}{C_f} \cdot 100\,\%, \tag{6}$$

where C_f and C_p is the content of solid particles in the initial mixture and permeate.

2. Discussion of the results

As a result of synthesis in a laboratory chamber electric furnace at temperatures of 800 °C–1300 °C porous ceramic materials based on SiC_P were obtained.

Structural studies of synthesized porous ceramic materials based on SiC_P filler powders have shown that the resulting ceramic material has a developed heterogeneous porous structure (Fig. 3). At sintering temperatures of 800 °C–1000 °C, particles of SiC_P retained sharp edges, and the joints between them were small and thin. With an increase in the sintering temperature to 1100 °C–1300 °C, the formation of strong interparticle compounds intensified, which led to an increase in pore size while reducing the open porosity. It is clearly seen that after sintering to a temperature of 1100 °C and above, SiC_P grains have small edge reflow effects, and between them are visible cast

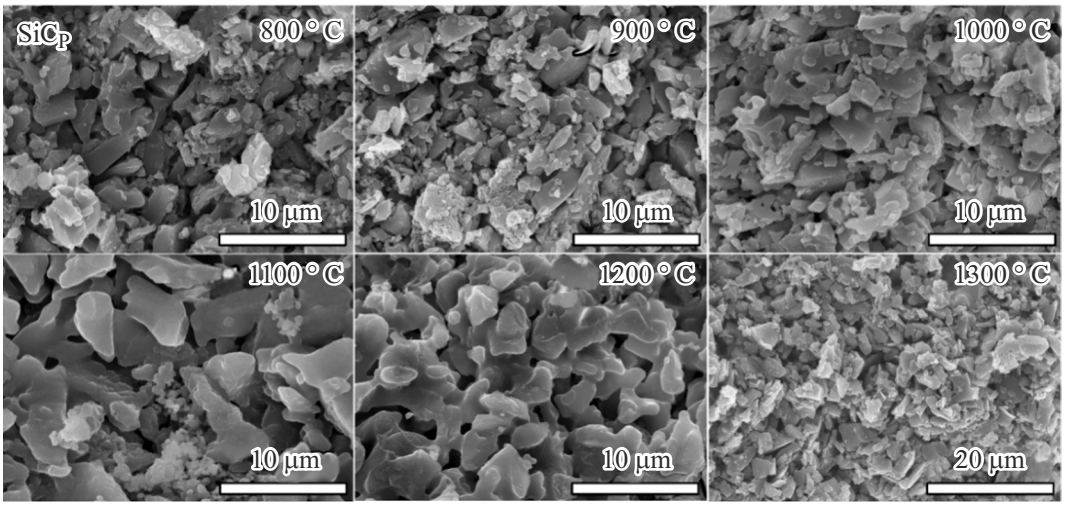

Figure 3. Microstructure of porous ceramic SiC materials.

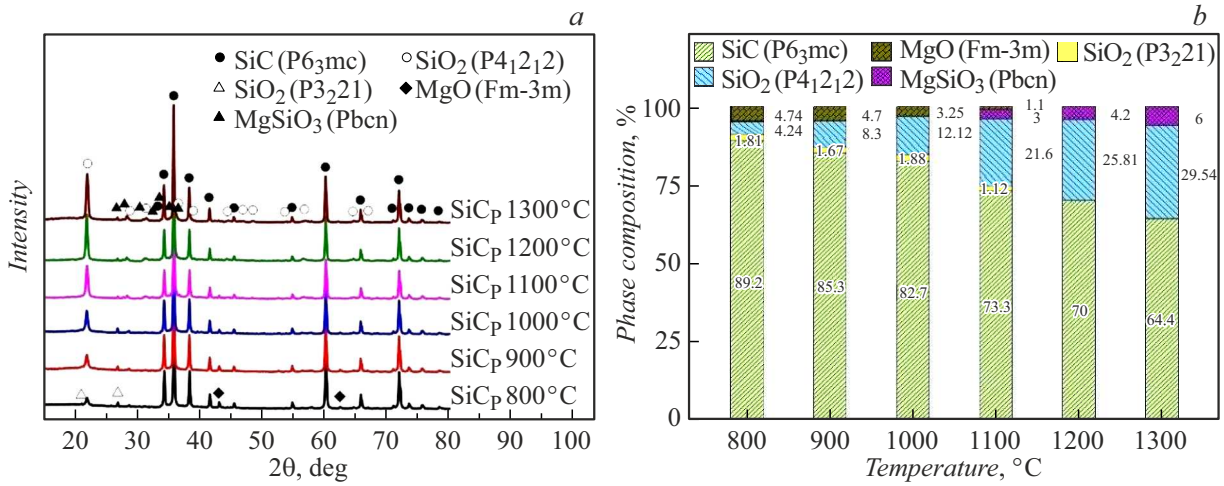

Figure 4. Diffraction pattern (a) and histogram of quantitative analysis (b) of porous ceramic SiC materials.

structures enveloping them, formed during sintering in the liquid phase with the participation of binding additives MgO and SiO_2.

Fig. 4, *a* shows diffractograms of a series of samples depending on the sintering temperature. The phase composition of the obtained porous materials is similar to SiC_{SHS} from Ref. [2] and can be described as a combination of two main phases, SiC and SiO_2, in various crystalline modifications.

At a temperature of 800 °C, the main phase of the product is the initial SiC (α-SiC). Weak reflexes corresponding to the phases of: cristobalite have also been recorded (PDF-2№ 010-77-8621, sp. gr. $P4_12_12$), α — quartz (PDF-2№ 010-77-1317, sp. gr. $P3_221$) and MgO (PDF-2№ 010-75-1525, sp. gr. $Fm\bar{3}m$). With a further increase in temperature to 1300 °C, an increase in cristobalite and clinoenstatite reflections is observed with a corresponding decrease in the intensity of SiC phase reflections.

Fig. 4, *b* shows the results of quantitative phase analysis for a series of samples of SiC_P. It is shown that during sintering (T_{max} = 800 °C–1300 °C), the proportion of SiO_2 increases significantly as a result of SiC oxidation, the higher the temperature and the initial specific surface area (it reached a maximum of 29.5 mass% at 1300 °C for SiC_P).

The oxidation of SiC_P samples gradually increases as the temperature increases. The lower degree of oxidation of SiC_P compared to SiC_{SHS} [2] is associated with a significant difference in the specific surface area of the filler powder particles, since the reactivity is directly proportional to the specific surface area of the filler powder.

Thus, based on the research results and the data of Ref. [2,5] reveals the principle underlying the sintering mechanism of powder mixtures of a similar composition. At the initial stage of sintering, primary bonds are formed

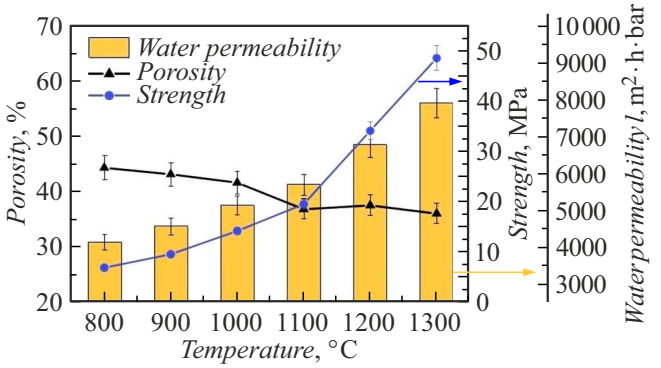

Figure 5. Open porosity, flexural strength, and permeability of synthesized materials.

between the particles of the initial powder mixture and the number of contacts between them increases. Then, the contact zones between the particles that appeared at the initial stage increase in size due to surface diffusion. The oxidation of silicon carbide accelerates at temperatures above 800 °C to form an active SiO_2. At sintering temperatures from 1100 °C, it begins to dissolve the MgO present in the additive to form a liquid phase of clinoenstatite composition [6], which moistens the surface of the aggregate grains. Clinoenstatite $MgSiO_3$ crystallizes in case of cooling, forming a strong framework of the porous material structure, which is confirmed by a significant increase in strength.

With an increase in the sintering temperature from 800 °C to 1300 °C, the bending strength of SiC_P membranes increased from 7.05 to 48.54 MPa, which is on average twice the strength of samples based on SiC_{SHS} synthesized at identical temperatures. The open porosity decreased from 44.28 % to 36.17 % (Fig. 5). At the same time, the water permeability of membranes based on SiC_P increases from 4125 to 7890 $l \cdot m^{-2} \cdot h^{-1} \cdot bar^{-1}$, which is on average 20 % higher than the water permeability of membranes based on SiC_{SHS} from Ref. [2].

An increase in water permeability is associated with a significant increase in pore size with an increase in sintering temperature, despite a decrease in open porosity, since it is the pore size that significantly affects the flow rate through the membrane than its porosity.

The measured linear thermal expansion of samples from materials based on SiC_P did not exceed 2.5 %. An increase in the mass of samples of the order of 6.2 mass% was also detected, which is associated with the formation of additional silicon oxide in the material during synthesis. It should be noted that the intensity of the increase in the mass of the samples decreases as the temperature increases. This indicates a decrease in the oxidation rate of SiC membranes with increasing sintering temperature, which is explained by the crystallization of the oxide layer and, consequently, a significant deterioration in the penetration of molecular oxygen through crystallized silica [7].

The gas permeability was also calculated based on the results of measurements of air flow rates through samples made of porous ceramic materials (Fig. 6). The maximum gas permeability was 0.084 μm^2 for samples sintered at 1300 °C, and the minimum gas permeability was 0.008 μm^2 for samples sintered at a temperature of 800 °C. The observed increase in permeability is symbiotic with an increase in water permeability, since the correlation with the pore size is obvious. The revealed difference between liquid and gas permeability is associated with lower viscosity and greater compressibility of the transmitted substance flow.

The synthesized materials were studied by mercury porometry and bubble point methods. Additionally, the pore size was estimated based on the results of measurements of gas permeability, the main results are presented in Table 1.

It was found using mercury porometry, that the synthesized samples have a unimodal pore size distribution (Fig. 7). It was found that the filler SiC_P with a low specific surface area forms a material with pores with sizes from 0.2 to 1 μm. There are practically no nanoscale pores in the SiC_P-based material.

The results of mercury porometry are symmetrical to the results of calculations of pore sizes based on gas permeability, as well as an estimate of equivalent hydraulic channel diameters measured by the bubble point method according to GOST 26849-86 (Fig. 8).

Membranes based on SiC_P have 20 % larger average pore sizes with a narrow distribution and, as a result, greater permeability than membranes based on SiC_{SHS} [2]. In addition, a twofold difference in the strength properties of synthesized materials based on morphologically different fillers was revealed. The research results show that the use of powders of the same size, but of different surface morphology, leads to the production of materials with significantly different properties.

Table 2 presents the physico-mechanical characteristics of porous ceramic materials synthesized by various methods as a result of studies in Ref. [8–15]. The data are presented

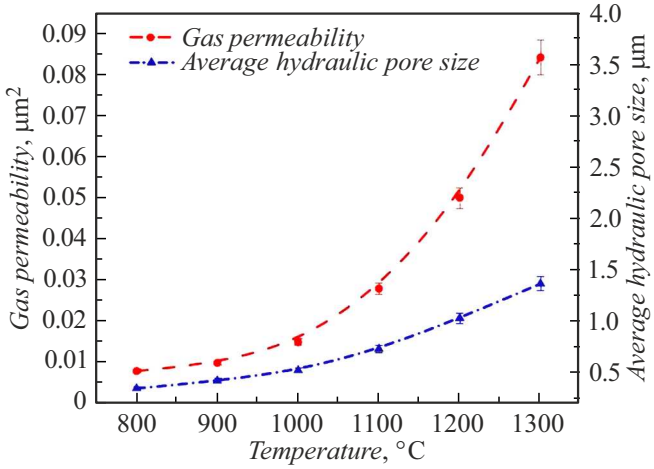

Figure 6. Gas permeability and average hydraulic pore size in ceramic materials based on SiC_P.

Table 1. The main characteristics of the pore structure of ceramics based on SiC

T, °C	General surface pores, m^2/g	Pore size (mercury porometry), nm	Pore size by gas-permeable permeability, nm	Pore size bubble point, nm	Strength, MPa	Porosity, %	Water permeability, $l \cdot m^{-2} \cdot h^{-1} \cdot bar^{-1}$	Tortuosity, RU
800	4.7	243 ± 12	350 ± 28	450 ± 42	6.8 ± 0.3	44.2 ± 2.2	4125 ± 206	30
900	4.2	410 ± 21	425 ± 34	620 ± 55	9.5 ± 0.5	43.1 ± 2.2	4551 ± 227	67
1000	2.4	568 ± 28	527 ± 42	720 ± 65	14.1 ± 0.7	41.6 ± 2.1	5123 ± 256	111
1100	1.9	649 ± 32	734 ± 59	850 ± 76	19.5 ± 0.9	36.8 ± 1.8	5684 ± 284	103
1200	1.5	728 ± 37	1030 ± 82	1050 ± 94	34 ± 1.7	37.5 ± 1.9	6765 ± 338	77
1300	1.1	977 ± 48	1367 ± 109	1240 ± 112	48.5 ± 2.5	36.0 ± 1.8	7890 ± 394	57

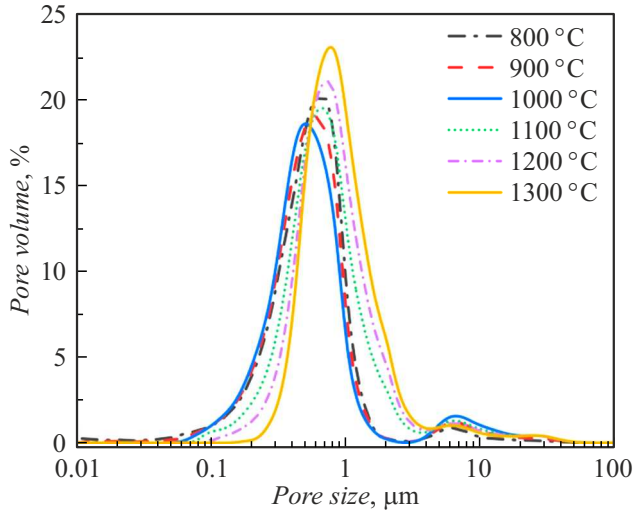

Figure 7. Pore size distribution in ceramic materials based on SiC_P.

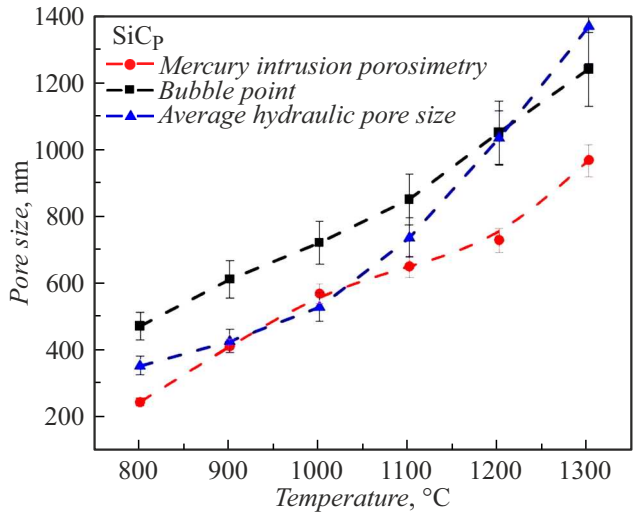

Figure 8. Comparison of the results of pore size determination in ceramic materials based on SiC_P by various methods.

in comparison with the characteristics of SiC_P-membranes synthesized in this study.

The maximum sintering temperature of porous ceramic materials based on SiC_P synthesized in this work was 1300 °C, which is lower than the sintering temperature of ceramics prepared from Al_2O_3 [8,9] and other materials [10,11]. Thus, energy efficiency is significantly increased and the cost of synthesis is reduced. At sintering temperatures up to 1000 °C, the open porosity of membranes based on SiC_P was similar to other materials presented, and the permeability to pure water was significantly higher than permeability to pure water of SiC-ash membranes [12] and SiC-coal ash [13].

In cases where the pore size is equivalent, the permeability of pure water through synthesized SiC membranes was higher by 10 %–15 %, and the mechanical strength was higher from 10 % to 50 % than that of [14,15]. Thus, the synthesized SiC membranes have demonstrated excellent integrated characteristics in terms of production cost, mechanical and operational properties, which makes them highly competitive for commercial use in filtration processes.

The effectiveness of synthesized membranes filtration processes was determined to evaluate their operational characteristics.. A suspension consisting of distilled water with a content of model SiC particles at the level of 2 mass% at particle sizes of $D_{50} = 0.5\,\mu$m was used as the filtrate.

In the course of the study, it was found that the permeate obtained was pure and transparent, and the calculated rejection coefficient showed more than 99 % efficiency of particle rejection from the suspension. During long-term operation, the membrane's performance did not fall below 50 % of the initial value. Additionally, the membrane was completely regenerated many times by ultrasonic cleaning, and upon repeated filtration, permeability and productivity were restored (up to 99 % of the original).

The results obtained indicate that the synthesized SiC membranes have high filtration efficiency while maintaining the stability of filtration characteristics during multiple model operational studies. In addition, they have sufficient

Table 2. Physical and mechanical characteristics of porous ceramic materials

Material	Temperature synthesis, °C	Porosity open, %	Pore size, μm	Strength bend, MPa	Water permeability, $l \cdot m^{-2} \cdot h^{-1} \cdot bar^{-1}$
Al_2O_3 [9]	1500	39	2.42	46.2	45 400
Al_2O_3 [10]	1400	41.4	6.8	32.7	45 000
SiC-Al_2O_3 [11]	1400	38.22	3.70	38.47	4417 – 4755
SiC-MgO [12]	1400	42.11	2.98	41.29	–
SiC-ash [13]	1000	36.40	2.90	38.40	1532
SiC-coal ash [14]	1000	44.7	3.7	28.6	5261
SiC-clay [15]	1200	54.3	0.95	$\sim$ 17.5	7000
Ash [16]	1150	42	0.49	26.6	5616
SiC_P	1000–1300	42–36	0.7–1	14.1–48.5	5100–7890

strength to withstand multiple cycles of mechanical forced regeneration.

Conclusion

Porous ceramic materials based on SiC_P were obtained using an energy-efficient method using low sintering temperatures (from 800 °C to 1300 °C). A direct dependence of the amount of synthesized SiO_2 in materials on the maximum sintering temperature has been established. The total proportion of SiO_2 for synthesized materials is about 29.5 mass% at a temperature of 1300 °C. The research results showed that the optimal sintering temperature of the investigated system with binders MgO and SiO_2 is in the range from 1000 °C to 1300 °C.

The open porosity decreases from 44 % to 36 % with an increase in the maximum sintering temperature. At the same time, the water permeability for membranes based on SiC_P increases from 4125 to 7890 $l \cdot m^{-2} \cdot h^{-1} \cdot bar^{-1}$, which is associated with a significant increase in pore sizes with increasing sintering temperature and the dominant influence of these sizes on the permeability of materials, despite a decrease in their open porosity. The water permeability of SiC_P membranes is on average 20 % higher than the water permeability of membranes based on SiC_{SHS}. Also, SiC_P membranes have high bending strength (up to 48 MPa), their strength properties are on average twice as high as the strength of samples based on SiC_{SHS} synthesized at identical temperatures.

The use of three different pore size measurement methods revealed the symmetry of their results, the differences between them are not fundamental. This is due to the fact that the particles of the filler material SiC_P, which have a fragmented structure and a low specific surface area, provide the formation of porous ceramics with a monomodal pore size distribution.

The determined filtration efficiency of porous ceramics was about 99 % when solid particles were rejected from the model suspension to ensure permeate purity. The synthesized SiC_P membranes showed the stability of filtration characteristics during multiple model operational studies. Repeated cycles of mechanical forced regeneration did not lead to deterioration of strength and operational properties.

The results of studies show that the use of powders of the same size, but with different morphology of their structure, leads to the production of materials with significantly different properties. Ceramic membranes synthesized using furnace powder SiC_P have higher permeability, pore size of $\sim 0.5 - 1\mu$m and their narrow distribution. This set of characteristics is suitable for their use in liquid microfiltration.

Conflict of interest

The authors declare that they have no conflict of interest.

References

[1] V.I. Uvarov, R.D. Kapustin, A.O. Kirillov, A.S. Fedotov, M.V. Tsodikov. Refract. Ind. Ceram., **61**, 355 (2020). DOI: 10.1007/s11148-020-00486-0
[2] A.O. Kirillov, R.D. Kapustin, V.I. Uvarov, O.D. Boyarchenko. Int. J. Self-Propag. High-Temp. Synth., **33** (4), 280 (2024). DOI: 10.3103/S1061386224700262
[3] V. Petrícek, M. Duček, L. Palatinus. Zeitschrift Fur Krist., **229** (5), 345 (2014). DOI: 10.1515/zkri-2014-1737
[4] N.T. Andrianov, V.L. Balkevich, A.V. Belyakov. *Praktikum po himicheskoj tekhnologii keramiki: uchebnoe posobie dlya vuzov* (OOO RIF „Strojmaterialy“, M., 2005)
[5] Z.Y. Luo, W. Han, X.J. Yu, W.Q. Ao, K.Q. Liu. Ceram. Int., **45**, 9007 (2019). DOI: 10.1016/j.ceramint.2019.01.234
[6] R.D. Kapustin, V.I. Uvarov, A.O. Kirillov. Open Ceram., **16**, 100499 (2023). DOI: 10.1016/j.oceram.2023.100499

[7] J. Rodríguez-Viejo, F. Sibieude, M.T. Clavaguera-Mora, C. Monty. Appl. Phys. Lett., **63** (14), 1906 (1993). DOI: 10.1063/1.110644
[8] Y. Cheng, Y. Yu, C. Peng, J. Wu. Ceram. Int., **46** (8), 11297 (2020). DOI: 10.1016/j.ceramint.2020.01.158
[9] H. Qi, Y. Fan, W. Xing, L. Winnubst. J. Eur. Ceram. Soc., **30** (6), 1317 (2010). DOI: 10.1016/j.jeurceramsoc.2009.12.011
[10] D. Das, N. Kayal, G.A. Marsola, L.A. Damasceno, M.D. de M. Innocentini. Int. J. Appl. Ceram. Technol., **17**, 893 (2020). DOI: 10.1111/ijac.13463
[11] C.Y. Bai, X.Y. Deng, J.B. Li, Y.N. Jing, W.K. Jiang, Z.M. Liu, Y. Li. Ceram. Int., **40** (4), 6225 (2014). DOI: 10.1016/j.ceramint.2013.11.078
[12] D. Das, K. Nijhuma, A.M. Gabriel, G.P.F. Daniel, D. de M.I. Murilo. J. Eur. Ceram., Soc., **40**, 2163 (2020). DOI: 10.1016/j.jeurceramsoc.2020.01.034
[13] D. Das, N. Kayal, M.D. de M. Innocentini. Trans. Indian Ceram. Soc., **80** (3), 186 (2021). DOI: 10.1080/0371750X.2021.1934122
[14] S.Z.A. Bukhari, J.H. Ha, J. Lee, I.H. Song. Ceram. Int., **43** (10), 7736 (2017). DOI: 10.1016/j.ceramint.2017.03.079
[15] D. Liang, J. Huang, Y. Zhang, Z. Zhang, H. Chen, H. Zhang. J. Eur. Ceram. Soc., **41** (11), 5696 (2021). DOI: 10.1016/j.jeurceramsoc.2021.04.055

Translated by A.Akhtyamov